Water vapor sounding with the far infrared REFIR-PAD spectroradiometer from a high-altitude ground-based station during the ECOWAR campaign

G. Bianchini,[1] L. Palchetti,[1] G. Muscari,[2] I. Fiorucci,[2] P. Di Girolamo,[3] and T. Di Iorio[4]

Received 25 May 2010; revised 20 November 2010; accepted 1 December 2010; published 28 January 2011.

[1] The Radiation Explorer in the Far InfraRed-Prototype for Applications and Development (REFIR-PAD) spectroradiometer was operated from the Testa Grigia Italian-Alps station in March 2007 during the Earth Cooling by Water Vapour Radiation (ECOWAR) measurement campaign, obtaining downwelling radiance spectra in the 100–1100 cm^{-1} range, under clear-sky conditions and in the presence of cirrus clouds. The analysis of these measurements has proven that the instrument is capable of determining precipitable water vapor with a total uncertainty of 5–7% by using the far-infrared rotational band of water. The measurement is unaffected by the presence of cirri, whose optical depth can be instead retrieved as an additional parameter. Information on the vertical profiles of water vapor volume mixing ratio and temperature can also be retrieved for three altitude levels. The ability to measure the water vapor column with a simple, uncooled instrument, capable of operating continuously and with a time resolution of about 10 min, makes REFIR-PAD a very valuable instrument for meteorological and climatological studies for the characterization of the water vapor distribution.

Citation: Bianchini, G., L. Palchetti, G. Muscari, I. Fiorucci, P. Di Girolamo, and T. Di Iorio (2011), Water vapor sounding with the far infrared REFIR-PAD spectroradiometer from a high-altitude ground-based station during the ECOWAR campaign, *J. Geophys. Res.*, *116*, D02310, doi:10.1029/2010JD014530.

1. Introduction

[2] Water vapor is a key atmospheric component that must be measured with great accuracy for both meteorological applications and climatological studies. Due to its intense absorption bands, water vapor plays an important role in the Earth radiation balance [*Kiehl and Trenberth*, 1997]. A better understanding of the water vapor climatological behavior requires the characterization of its atmospheric concentration at different altitudes and in different sky and atmospheric conditions. The precipitable water vapor (PWV), i.e., the column amount of water vapor present in the atmosphere, or the vertical profile of concentration can also be used to develop and validate atmospheric models [*Clough et al.*, 1992; *Delamere et al.*, 2010].

[3] The vertical distribution of water vapor is typically measured for meteorological applications by using radiosounding systems. Although such measurements can also be used for climate studies [*Elliott and Gaffen*, 1991], they are limited by accuracy [*Vömel et al.*, 2007] and by a low measurement repetition rate which prevents the proper characterization of rapidly changing atmospheric phenomena. Other measurement methods exploit the spectral features of water vapor either using passive spectroscopy, from microwave to infrared spectral regions [*Tobin et al.*, 1999; *Divakarla et al.*, 2006], or using active Raman lidars [*England et al.*, 1992; *Di Girolamo et al.*, 2009] and DIALs [*Bösenberg*, 1998].

[4] In this paper we describe the inversion method developed to retrieve the PWV and the vertical profiles of water vapor and temperature from the spectrally resolved downwelling atmospheric radiance acquired in the far-infrared region of the pure rotational water vapor band. These measurements were performed by the Radiation Explorer in the Far-Infrared-Prototype for Applications and Development (REFIR-PAD) spectroradiometer [*Bianchini et al.*, 2006], which was developed in the framework of the REFIR studies [*Palchetti et al.*, 1999; *Rizzi et al.*, 2001; *Palchetti et al.*, 2005], for the characterization of the Earth's emitted radiance from the far-infrared to midinfrared spectral region [*Sinha and Harries*, 1995].

[5] The REFIR-PAD instrument is a Fourier transform spectroradiometer designed to operate both from balloon platform, in the nadir and limb view observation geometries [*Palchetti et al.*, 2006, 2007], and from the ground in the zenith looking geometry [*Bianchini et al.*, 2007]. The instrument is characterized by a compact, uncooled design,

[1] Istituto di Fisica Applicata "Nello Carrara," Consiglio Nazionale delle Ricerche, Sesto Fiorentino, Italy.
[2] Istituto Nazionale di Geofisica e Vulcanologia, Rome, Italy.
[3] Dipartimento di Ingegneria e Fisica dell'Ambiente, Università della Basilicata, Potenza, Italy.
[4] Dipartimento di Fisica, Università di Roma "La Sapienza," Rome, Italy.

0148-0227/11/2010JD014530

Table 1. REFIR-PAD Instrument Main Characteristics

Characteristics	
Instrument type	Mach-Zehnder nonpolarizing FTS
Beam splitter	Broadband Ge-coated Mylar
Operating spectral bandwidth	100–1100 cm^{-1}
Operating spectral resolution	0.5 cm^{-1} (unapodized, double-sided)
Optical throughput	0.01 cm^2 sr
Field of view	133 mrad
Detector type	Room temperature pyroelectric (DLATGS)
Acquisition time	30 s per scan
Weight	55 kg including control electronics
Power consumption	~50 W (24 VDC power supply)

with a misalignment-compensated optical scheme that can provide wideband (100–1100 cm^{-1}) atmospheric emission spectra with a 0.5 cm^{-1} spectral resolution (unapodized). REFIR-PAD main characteristics are summarized in Table 1.

[6] In March 2007 the instrument was operated from a ground station at the altitude of 3480 m a.s.l. during the Earth Cooling by Water Vapor Radiation (ECOWAR) campaign [*Bhawar et al.*, 2008]. A cross validation among the PWV values retrieved with the REFIR-PAD measurements and the PWV values measured with the other sensors deployed in the campaign (radiosondes, a Raman lidar and a millimeter-wave spectrometer) was already performed but only for few measurements in coincidence with the radiosonde launches [*Fiorucci et al.*, 2008]. In this paper we perform an in-depth analysis by comparing all the available PWV data with a maximum temporal resolution of 10 min. This improved resolution with respect to previous work [*Fiorucci et al.*, 2008] further underlines the high accuracy of the PWV data sets presented, with particular emphasis to our newly developed algorithm applied to the REFIR-PAD spectral measurements in the far-IR.

2. Field Campaign

[7] The ECOWAR campaign was performed from Testa Grigia station of the Italian Consiglio Nazionale delle Ricerche (CNR) on Plateau Rosa (3480 m a.s.l., 45.933°N, 7.7°E), 5 km apart from Breuil-Cervinia (1990 m a.s.l., 45.933°N, 7.6°E) in the Italian-Swiss Alps near Aosta.

[8] REFIR-PAD was installed at Testa Grigia in a heated and thermally insulated enclosure just outside the station (see Figure 1). The instrument optical input port had no windows and thus was protected by a chimney to avoid deposition of ice crystals transported by the wind on the input optics.

[9] The instrument was operated for a total of 61 h, with measurements distributed across 11 days, including daytime and nighttime, with widely varying meteorological conditions both in terms of water vapor concentration and the presence of cirrus clouds. Table 2 reports the date, time and sky condition for all the measurements acquired.

[10] The correlative measurements used for the cross validation of the parameters retrieved from the REFIR-PAD measurements are: (1) PWV measured by the Ground-Based Millimeter wave Spectrometer (GBMS), designed and built

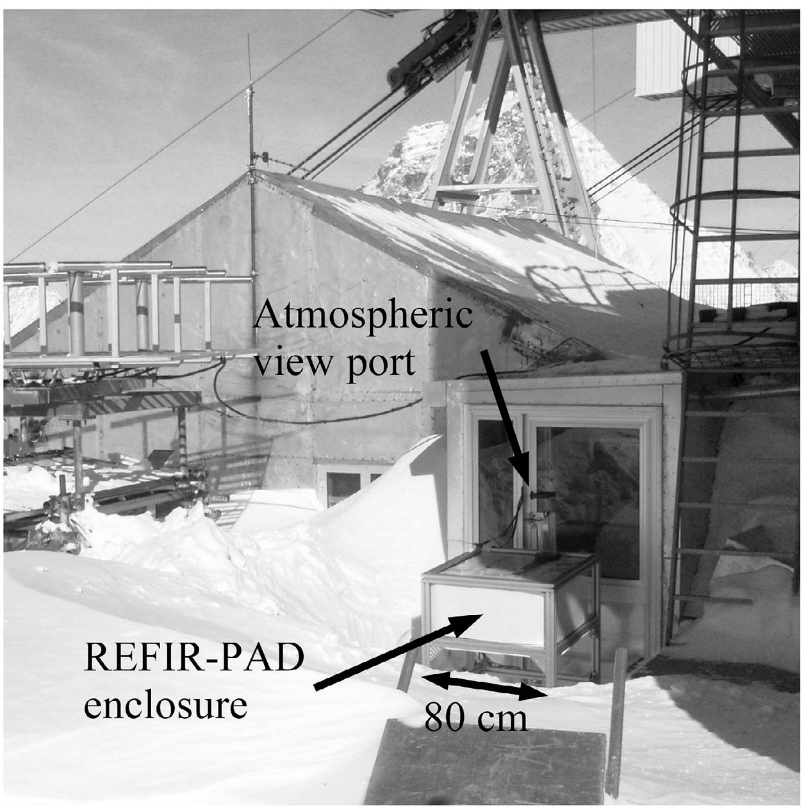

Figure 1. The REFIR-PAD instrument installed outside the Testa Grigia station at 3480 m a.s.l. in the Italian-Swiss Alps.

Table 2. Data Available From the ECOWAR Campaign[a]

Site	Date	Time (UTC)	Sky Conditions
TG	4 March 2007	1920–2339	cirrus (8–12 km)
TG	5 March 2007	1754–0043 (+1 d)	clear/cirrus
TG	9 March 2007	0725–1353	cirrus (7–11 km)
TG	11 March 2007	1622–0206 (+1 d)	clear
TG	12 March 2007	0844–1545	clear
TG	12 March 2007	1755–2302	clear
TG	13 March 2007	0915–1403	clear
TG	13 March 2007	1821–0804 (+1 d)	clear
BC	15 March 2007	1514–2309	clear

[a]TG, Testa Grigia station; BC, Breuil-Cervinia; +1 d in the Time column denotes that measurements extended to the following day.

at the Physics and Astronomy Department of the State University of New York at Stony Brook, and operated on Testa Grigia site by the Istituto Nazionale di Geofisica e Vulcanologia [*Fiorucci et al.*, 2008]; (2) vertical profiles of water vapor concentration and temperature measured by the University of Basilicata Raman lidar system (BASIL), developed in collaboration between the University of Rome "La Sapienza" and the University of Basilicata and installed at Breuil-Cervinia [*Di Girolamo et al.*, 2004]; and (3) vertical profiles of water vapor concentration and temperature measured by Vaisala RS92k radiosondes launched from Breuil-Cervinia [*Miloshevich et al.*, 2004].

[11] On 15 March the REFIR-PAD was transferred down to Breuil-Cervinia to perform simultaneous colocated measurements with the sensors present there, in particular the BASIL lidar and the Fourier transform infrared (FTIR) ABB Bomem spectroradiometer [*Serio et al.*, 2008].

[12] More information on the whole set of measurements and on the comparison with the FTIR/ABB spectroradiometer is provided by *Bhawar et al.* [2008].

[13] The main REFIR-PAD level 1 data product is the calibrated downwelling spectral radiance, measured in the 100–1100 cm^{-1} spectral range with a 0.5 cm^{-1} resolution, although, for ground-based measurements, atmospheric water vapor absorption sets a low-frequency limit to the useful range to about 250–350 cm^{-1}. The level 1 data analysis, including calibration issues and uncertainty characterization, is treated elsewhere [*Bianchini and Palchetti*, 2008].

[14] During the ECOWAR campaign, the instrument was operated only under visually clear sky conditions, so the only cloud type that is of some concern in the analysis of REFIR-PAD data is thin/subvisible cirrus. Values of PWV lower than 0.5 mm were detected, with a typical value of about 2 mm and peak values of 3–4 mm. In Figure 2, two measured spectra are shown, in two extreme cases, 0.5 mm and 3 mm of PWV.

[15] Different conditions were detected also in terms of water vapor variability, with days characterized by extremely stable PWV over hours and days characterized by strong PWV variability during which the REFIR-PAD capability of continuous measurements with high temporal resolution was tested.

3. Atmospheric Variables Retrieval

[16] The level 2 analysis of the calibrated spectral radiances was performed through the best fitting of an atmospheric forward model with respect to a chosen subset of atmospheric parameters. These include one to four altitude levels on which the water vapor and temperature profiles are interpolated, cloud extinction coefficient, and instrumental parameters like line shape correction and frequency calibration factors. The latter will be treated in section 4, while cloud parameterization is described in section 5.

[17] The forward model used in the analysis is the Line-By-Line Radiative Transfer Model (LBLRTM) from AER Inc. [*Clough et al.*, 2005; *Shephard et al.*, 2009]. The model choice was driven by a number of features that are needed for the REFIR-PAD data analysis and that are provided by LBLRTM: (1) an up-to-date spectroscopic database (AER v. 2.2) including HITRAN 2004 and successive updates [*Rothman et al.*, 2005; *Gordon et al.*, 2007], (2) MT_CKD v. 2.4 self- and foreign-broadened water vapor and CO_2 continua (E. J. Mlawer et al., A revised perspective on the water vapor continuum: The MT CKD model, manuscript in preparation, 2010), and (3) modeling of CO_2 line coupling and updates to CO_2 continuum and line shape according to [*Niro et al.*, 2005].

[18] The best fit is obtained through a χ^2 minimization routine without a priori constraints on the parameters, except for the physical upper and lower limits on some of these parameters, namely water vapor and cloud extinction coefficient. This is done in order to avoid any anomalous behavior and the consequent convergence problems that are due to nonphysical parameter guesses that could be given by the minimization routine: for example, negative water vapor volume mixing ratio (VMR) values could be provided in very dry atmospheric conditions. These limits were chosen to be about 2 orders of magnitude below (lower limit) or above (upper limit) both actual fitting results and the entire ensemble of the radiosoundings performed from Breuil-Cervinia during the campaign, so do not provide a source of external information to bias the results.

[19] The χ^2 is calculated on the whole selected spectral interval, without microwindow selection, and is provided, as a function of the fitted parameters, to the MINUIT minimization routine [*James*, 1994]. The MINUIT software makes function calls to the LBLRTM model and performs χ^2 calculation in function of the values of the fitted parameters during minimization iterations. When convergence criteria are met, the iteration is stopped and final parameter values are output. A flowchart depicting the fitting process is shown in Figure 3.

[20] Among the atmospheric variables showing signatures in the REFIR-PAD operating range, we concentrated our attention on water vapor and temperature, so the actual spectral range that is used in the analysis is a subinterval of the REFIR-PAD operating band, range which extends from about 400 to 850 cm^{-1}. In this spectral region the retrieval is sensitive to water vapor vertical distribution from the rotational band in the far-infrared [*Bianchini et al.*, 2007], temperature vertical profile from the CO_2 v2 band and information on water vapor continuum and thin cirrus clouds from the transparent atmospheric window above 750 cm^{-1}.

[21] The retrieval of atmospheric structure from ground-based infrared measurements is generally ill-behaved due to the fact that the denser atmospheric layers appear first in the line of sight, reducing the sensitivity to upper layers. As a consequence, for each measurement channel the corre-

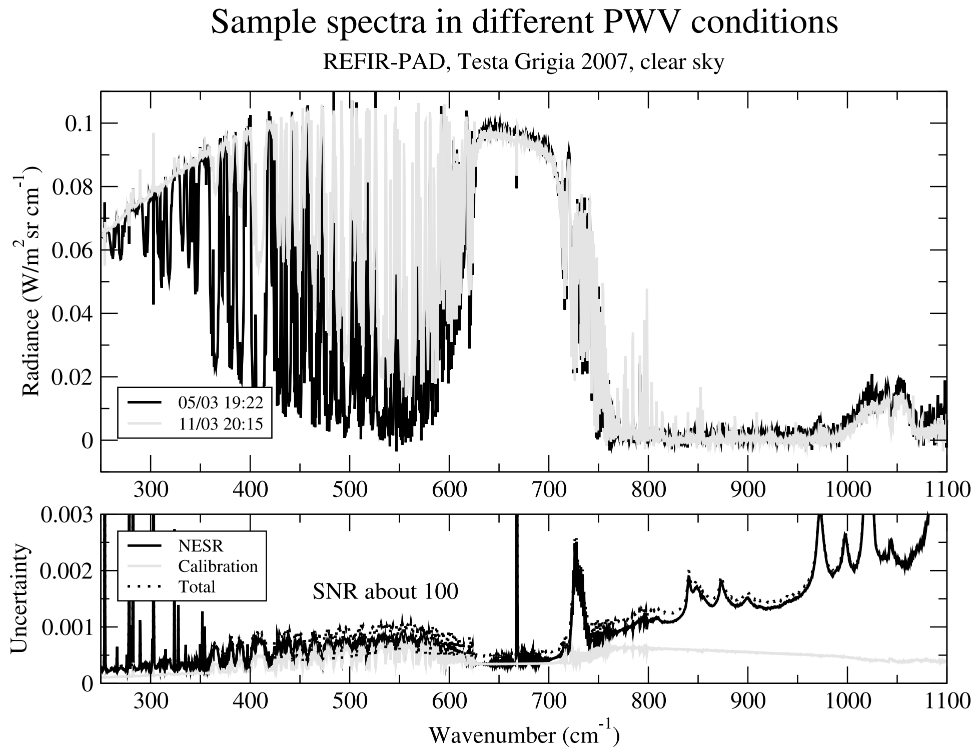

Figure 2. (top) Two REFIR-PAD calibrated downwelling radiance spectra acquired in different atmospheric conditions: 0.5 mm of PWV (black curve) and 3 mm of PWV (grey curve). (bottom) Measurement uncertainty: random (NESR), systematic (calibration), and total.

sponding weighting function has its maximum at the ground, and the sensitivity to atmospheric parameters extends only few kilometers above the ground [*Wang*, 1974].

[22] The choice of the atmospheric parameters to be used in the fit must take into account the vertical resolution provided by zenith-looking infrared sounding, that ranges from some hundreds of meters near ground to about 1 km above the altitude of 1 km [*Smith et al.*, 1999]. The initial choice for the vertical profile analysis is to fit a water vapor and temperature value at 1 km above ground, and a second point at 3 km above ground. Levels of the profiles between the two fitted points are interpolated (logarithmically for water vapor and linearly for temperature), while levels above and below fitted points are obtained by rescaling the midlatitude winter standard atmospheric profiles accordingly to the fitted values.

[23] The possibility of fitting three and four levels per profile, adding one or two near ground level for both water vapor and temperature, thus exploiting the higher information content of the lower levels [see *Smith et al.*, 1999] was also explored. In the three-level case, a fitted point at ground is added, in the four-level case another point at 50 m above ground is added to take into account for the possibility of an inversion layer.

[24] Moreover, a fitting with only one parameter per profile (i.e., just rescaling standard profiles) was used to estimate the uncertainty on the total water column without being affected by correlation between fitted points (see section 6).

[25] It should be noted that the use of two fitted parameters per profile provides improved PWV values with respect to simple rescaled profiles due to better fitting of the actual atmospheric vertical structure, while the variation between PWV values obtained with three- and four-point fitting with respect to two-point fitting, if present, is well within uncertainty. Correlation between fitted points instead, increases and can cause profile instabilities. For this reason the use of more than four fitted parameters per profile appears to be difficult without the use of a priori constraints. As a consequence, the PWV values used for cross-validation purposes are obtained by the two-point fitting. In section 7 a more quantitative analysis of the differences between different fitting strategies is provided.

4. Deriving Instrument Parameters

[26] A subset of the fitting parameters is used to take into account systematic effects due to the characteristics of the instrument. These parameters are: (1) a frequency scale calibration factor and (2) an apodization effect on the instrumental line shape (ILS).

[27] As described by *Bianchini and Palchetti* [2008], frequency calibration of REFIR-PAD spectra is performed using as a reference atmospheric line centers. This procedure does not need to be performed more often than on a daily basis due to the intrinsic stability of the laser frequency reference. It is possible anyway that some small changes in laser frequency happen, both due to laser diode aging and to the extreme thermal excursions that can be experienced during measurement campaigns. To avoid performing a calibration on a per spectrum basis, as could be required in these cases, a frequency shift factor was included in the

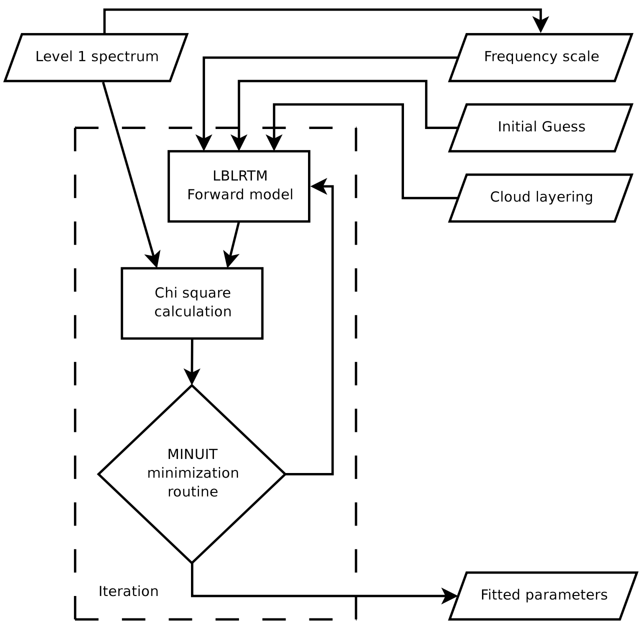

Figure 3. Flowchart of the fitting procedure used to retrieve atmospheric parameters from REFIR-PAD spectra. The MINUIT software makes use of the LBLRTM model as a function call to perform χ^2 calculation in function of parameter values. When convergence criteria are met, the iteration is stopped and final parameter values are output.

fitted parameters. This factor does not affect in any way the retrieval of atmospheric variables since is almost completely uncorrelated with them.

[28] Interferometer misalignments may be caused by thermal excursions. The loss of signal associated with misalignment is well taken care of in the radiometric calibration procedure [see *Bianchini and Palchetti*, 2008], but the ILS variations that are associated to misalignments must be taken into consideration in the level 2 analysis. A first-order approximation of this effect is to assume a linear decrease in the fringe contrast with the variation of path difference, i.e., a trapezoidal apodization function. This translates into an ILS that is a linear combination of *sinc* and $sinc^2$ components. The percentage of pure *sinc* component is thus fitted as a separate parameter to provide line shape correction for misalignment. Even in this case the correlation with atmospheric parameters is low and can be neglected.

5. Treatment of Cirrus Cloud

[29] REFIR-PAD measurements are performed exclusively in clear sky conditions, since the presence of an opaque cloud layer prevents the retrieval of the full PWV. It is possible, anyway, that a light cloud cover appears during a measurement run. Of particular interest is the case of a thin, possibly subvisible, cirrus, a condition that actually has occurred a few times during the campaign.

[30] This kind of cloud is not easily detected visually, moreover it appears at altitudes that are well above the measurement sensitivity range identified in section 3 for the water vapor and temperature profiles. This opens the possibility to perform fitting, and provides an accurate measurement of the atmospheric variables, also in presence of thin clouds.

[31] The simple cloud model included in the LBLRTM software is derived from the LOWTRAN5 routines [*Kneizys et al.*, 1980] and provides modeling for standard and subvisible cirri. A single cloud layer can be identified by cloud bottom (CB), layer thickness and extinction coefficient expressed in km^{-1} at 0.55 μm.

[32] Only the extinction coefficient is determined, since fitting results are not dependent on cloud geometry if CB is higher than the water vapor/temperature sensitivity range. In fact, the latter, as shown in section 3, is 3–4 km above ground, and cirrus clouds are situated at higher altitudes.

[33] Figure 4 shows, as an example, the variability of the particle backscattering coefficient at 355 nm for the night of 4 March 2007 as measured by the BASIL lidar in Cervinia.

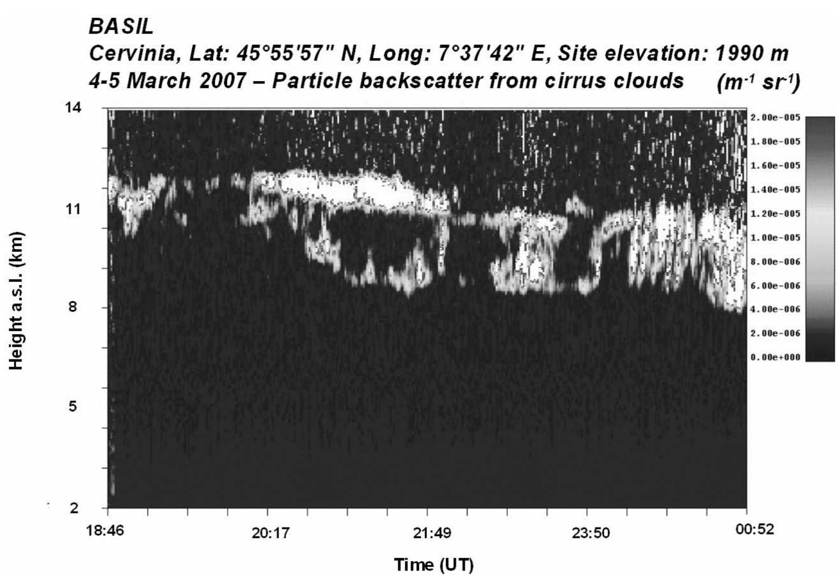

Figure 4. Backscatter plot acquired from the BASIL lidar at Cervinia on the night of 4 March 2007. Cirrus clouds at about 9–11 km are present during the whole acquisition period.

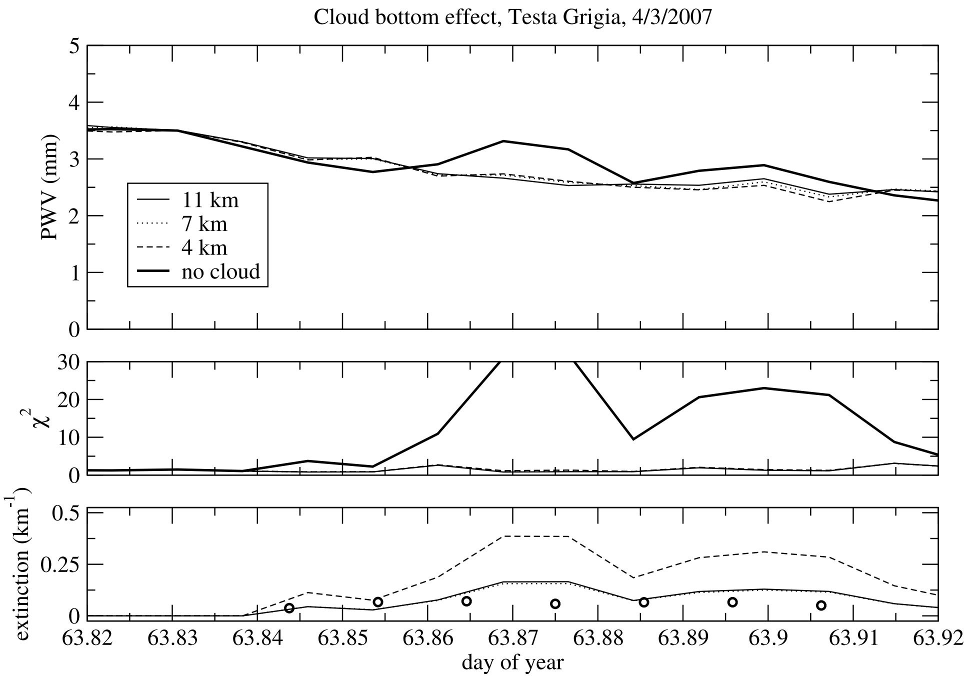

Figure 5. Effect of different cloud parameterizations on fitting results: a subvisible cirrus cloud layer 2 km thick with cloud bottom at 4 km (dashed line), 7 km (dotted line), and 11 km (solid line) was used. Results obtained without clouds (thick solid line) are also shown. (top) PWV and (bottom) cloud extinction values obtained from the fit; cloud extinction at 532 nm as measured by the BASIL lidar is also shown (as circles) for reference. (middle) The χ^2 values obtained from the fitting procedure.

In the plot a cirrus layer in the altitude region 9–11 km is clearly visible.

[34] Figure 5 shows the analysis of REFIR-PAD spectra acquired on the same day, performed both without cloud modeling (thick solid line) and with a modeled cloud layer of 2 km of thickness and CB heights of 4, 7 and 11 kilometers (dashed, dotted and solid lines, respectively). It is clearly visible that a fitting process without cloud modeling gives wrong, overestimated, PWV values (Figure 5, top) when cloud optical density is not negligible. The effect is even more evident in the χ^2 plot (Figure 5, middle).

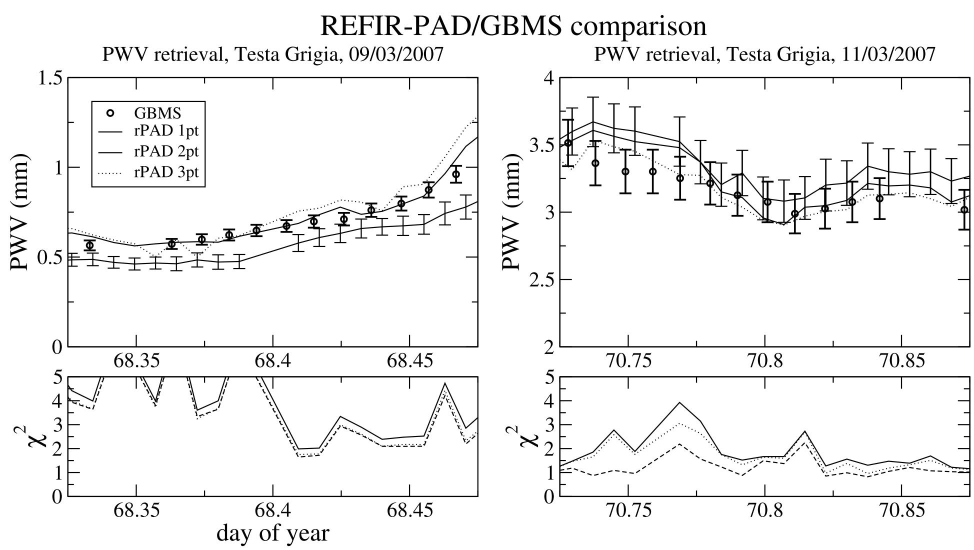

Figure 6. (top) Total precipitable water vapor (PWV) retrieved from REFIR-PAD spectra acquired on 9 and 11 March 2007 using one-, two-, and three-points fitting process (solid, dotted and dashed lines, respectively) and PWV values measured by the GBMS (circles). Since uncertainty is the same for the three different fitting strategies, error bars are shown only on the one-point measurements for better readability. (bottom) The χ^2 values obtained from the fitting of REFIR-PAD data.

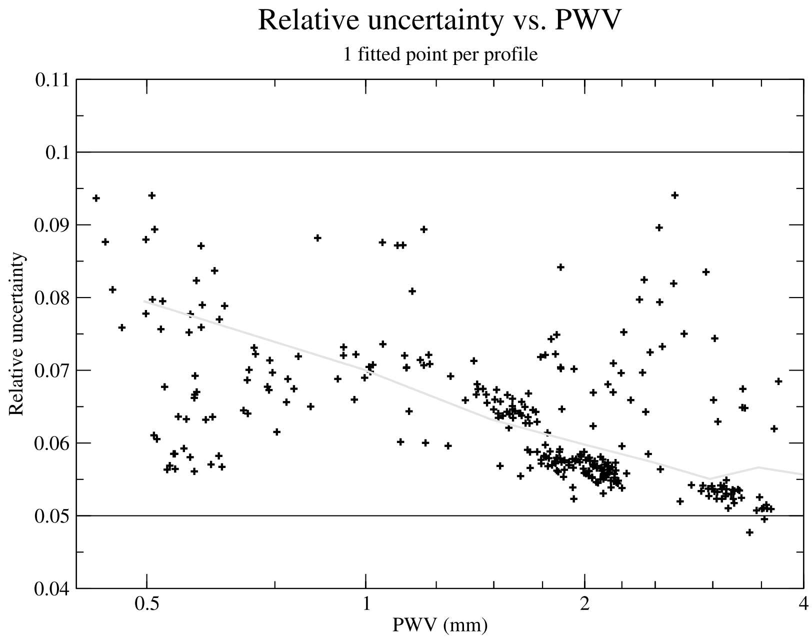

Figure 7. Relative uncertainty on PWV, as obtained from one-point fitting, plotted versus PWV itself to show relation between the two quantities.

[35] Figure 5 (bottom), showing the retrieved cloud extinction coefficient (evaluated at 550 nm), reveals that the difference between the retrievals performed with CB at 7 and 11 km is negligible; as explained before, this is to be attributed to the fact that the modeled cloud layer is situated above the water vapor/temperature sensitivity region. On the contrary, the curve corresponding to a CB of 4 km leads to large overestimated values.

[36] As a reference, cloud extinction at 532 nm as measured by the BASIL lidar is also shown in Figure 5 (bottom) (as circles), and provides a reasonable agreement with the REFIR-PAD retrieved values, considering the lack of an exact spatial coincidence between the two measuring stations.

6. PWV Measurement Uncertainty

[37] Due to some parameter correlation, the calculation of uncertainties on each of the fitted atmospheric variables that are obtained from this analysis depends on the number of points fitted per profile. However, the correlation does not affect the accuracy of PWV measurement since the correlation generally induces some degree of profile instability, in the form of oscillations, but that does not alter the retrieved total water column. This can be seen from the relatively small adjustments that occur in PWV retrieval using a different number of fitted parameters in the atmospheric profiles (Figure 6).

[38] A better estimate of the actual uncertainty affecting PWV measurement can thus be obtained from the relative uncertainty of the water vapor profile when fitting a single parameter per profile, i.e., just rescaling the initial guess. In Figure 7 is shown a plot of the relative uncertainty obtained with this method v. the retrieved PWV. Values are always below 10%, and most are between 5% and 7%.

[39] The behavior of the relative uncertainty with respect to the PWV can be modeled through an error analysis performed on synthetic spectra. For this task, downwelling radiance spectra are simulated with the same forward model used in the retrieval, with the midlatitude winter standard atmosphere water vapor vertical profile rescaled to provide different PWV values in the range 0.5–4 mm (the same as REFIR-PAD measurement at Testa Grigia) as input. Random noise with an RMS value corresponding to the total spectral uncertainty on the REFIR-PAD measurements is then added to the synthetic spectra to simulate instrumental noise.

[40] The relative uncertainty resulting from the analysis of the synthetic spectra is shown in Figure 7 as a grey line. These values are in good agreement with the uncertainties obtained from the analysis of measured spectra, with most of the points grouped near the calculated value and some spread that is explained by excess noise due to external causes (wind, for example, since the instrument was installed outside the research station).

[41] Effects associated with a possible correlation between the retrieved water vapor amount and the other fitted parameters in the one-point-per-profile analysis used to assess PWV uncertainty were estimated to be negligible. As shown in section 4, instrumental parameters are uncorrelated with atmospheric variables. The effect of the uncertainty on temperature profile rescaling, an operation that is needed since also temperature is a fitted parameter in the one-point analysis, was estimated and found to be at least an order of magnitude smaller than the uncertainty from the water vapor fitting, so it can also be neglected.

7. Results and Validation

[42] PWV values retrieved from the analysis of REFIR-PAD spectra were validated through the comparison with

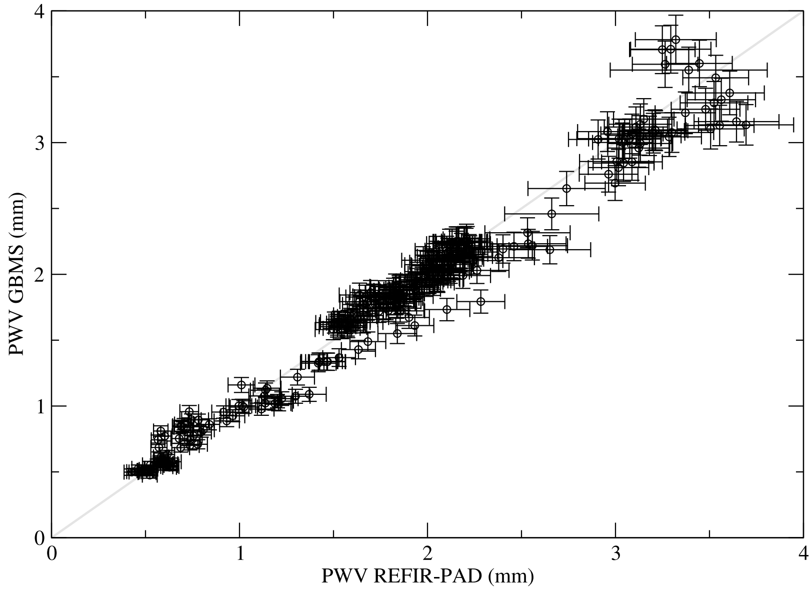

Figure 8. PWV measured from REFIR-PAD plotted versus PWV measurements performed in coincidence by the GBMS radiometer.

the values obtained from the GBMS instrument, operated at Testa Grigia near REFIR-PAD.

[43] The GBMS measures atmospheric emission spectra in the interval between 7.7 and 9.3 cm^{-1} with a maximum time resolution of 10 s. During the ECOWAR campaign measurements were averaged over a time intervals of 15 min, that is about the same acquisition time that is needed for a REFIR-PAD spectrum. The conversion of the microwave radiances to PWV is described by *de Zafra et al.* [1983] and *Fiorucci et al.* [2008].

[44] The spatial coincidence between the GBMS and the REFIR-PAD instruments was rather good, as the distance between them was only a few tens of meters. However it must be taken into account that while the REFIR-PAD operates in a zenith-looking observation geometry, the GBMS observes the atmosphere in a direction 10–15 degrees above the horizon. Considering this and the fact that most of the water vapor signal comes from the lower 3 km of the atmosphere, we can estimate the actual distance between the air masses sampled by REFIR-PAD and GBMS being less than 15 km.

[45] In Figure 6 is shown a comparison between the PWV values obtained from the GBMS (circles) and the values from REFIR-PAD (one-point fit: solid line, two-points fit: dotted line, three-points fit: dashed line). Two cases are considered, one with rather high (about 3 mm) and one with low (0.5 mm) precipitable water vapor content levels. The accuracy and time resolution of the two instruments are comparable and the results agree within uncertainties, for the two- and three-point fit. It should be noted that the one-point fit has a detectable offset from the GBMS value, showing that the use of more profile points adds information to the results.

[46] Figure 8 shows a scatterplot of all the REFIR-PAD PWV measurements, in the two-points fitting case, versus coincident GBMS values. Even in this case, the agreement is good within the uncertainty, and no significant bias is present. Similar plots in the three- and four-points case show a very similar behavior, with some small differences that are best identified through linear regression statistics, as shown in Table 3. It is interesting to note that while the correlation coefficient R slightly decreases with the increasing of the number of fitted points, the slope and intercept provided by the linear regression do actually improve. This is due to the fact that even if, on average, more points give a better fit of the atmospheric profile, the correlation between points increase the scatter of the data points and thus R.

[47] To assess the information on vertical water vapor profile that can be obtained from REFIR-PAD spectra, a comparison was also made with the BASIL lidar system. This system is capable of performing vertical soundings of water vapor mixing ratio and temperature, particle backscatter at 355, 532 and 1064 nm, and particle extinction and depolarization at 355 and 532 nm, based on the application of the Raman Lidar technique in the UV.

[48] Measurements are performed both during the daytime and the nighttime. For a time resolution of 5 min and a vertical resolution of 150 m, daytime measurement uncertainty at 2 km altitude is typically 5% for the particle backscattering coefficient (at all wavelengths), 20% for the particle extinction coefficient, 10% for water vapor mixing

Table 3. Linear Regression Statistics on the Correlation Between REFIR-PAD and GBMS Data in the Case of One-, Two-, Three-, and Four-Points Fit

Number of Points	Slope	Intercept	R
1	0.862 ± 0.013	0.178 ± 0.027	0.974
2	0.951 ± 0.010	0.063 ± 0.021	0.986
3	0.966 ± 0.012	0.031 ± 0.024	0.982
4	0.977 ± 0.012	−0.003 ± 0.025	0.981

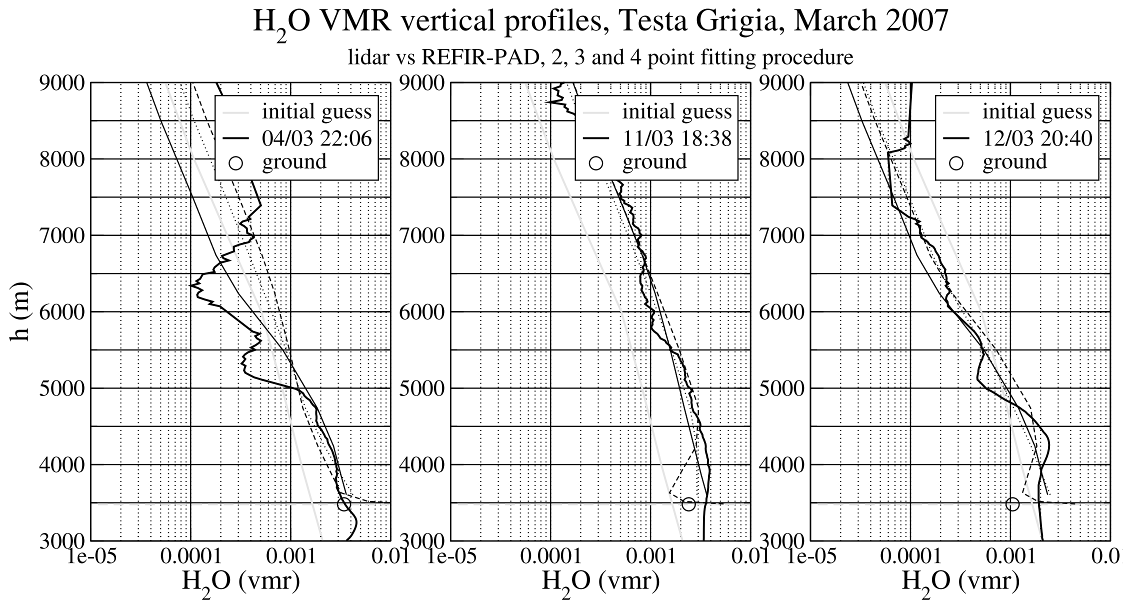

Figure 9. Water vapor vertical VMR profiles obtained from REFIR-PAD data through the two-points (solid line), the three-points (dotted line), and the four-points (dashed line) retrieval processes compared with coincident profiles measured by the BASIL lidar (thick line) on (left) 3 March, (middle) 3 November, and (right) 3 December. Groundwater vapor VMR measured from a Meteo station operating on the Testa Grigia site is also shown (circles).

ratio and 2 K for temperature. Nighttime measurement uncertainty at 2 km is typically 2% for the particle backscattering coefficient, 10% for the particle extinction coefficient, 5% for water vapor mixing ratio and 1 K for temperature.

[49] The horizontal distance between the REFIR-PAD and BASIL measurement sites was about 5 km, so considering that both have a vertical observation geometry we can expect a good correlation between the measurements.

[50] Figure 9 shows a comparison between three different lidar water vapor profiles acquired in different days of the campaign, and the corresponding REFIR-PAD retrieved profiles in the two-, three- and four-point fit cases. Since the lidar is operated from 1991 m a.s.l., at the altitude of the REFIR-PAD measuring site it is actually sampling the free troposphere. To take this into account and to show, if present, boundary layer effects, water vapor VMR values obtained from a meteorological station installed on the REFIR-PAD site is also shown in the plot.

[51] It should be noted that when the ground measurement differs significantly from the lidar profile, the four-points REFIR-PAD retrieval captures this feature approaching the ground measurement value with the lower layers, while the upper layers are in good agreement with the lidar profile.

[52] Due to the low vertical resolution, the REFIR-PAD retrieved profile is not able to reproduce the vertical structure present in Figure 9 (left), while in the case of smoother profiles (Figure 9, middle and right), the agreement is better, and it can be seen that there is a slight improvement in the agreement that is gained using the three-point rather than the two-point profile. The use of four fitting points does not provide useful improvement in the agreement with lidar profiles, since the resolution increase is obtained near the ground, where the REFIR-PAD measurements are sensitive to boundary layer effects that are not seen in the lidar sounding. Nevertheless, it should be noted that this extra information that is obtained on the layers near ground is in good agreement with atmospheric parameters measured by a colocated meteorological station.

8. Conclusions

[53] This paper has demonstrated the capability of the REFIR-PAD instrument to provide, besides the level 1 calibrated downwelling radiance spectra, also a variety of atmospheric parameters that are obtained through level 2 analysis of the atmospheric radiances.

[54] The main level 2 product is the precipitable water vapor, which is measured with a time resolution of about 10 min, and an accuracy between 5 and 7%.

[55] Information about the vertical profile of water vapor and temperature is also obtained, along with cloud extinction in the presence of thin high-altitude clouds (cirri).

[56] These capabilities, along with the characteristics of ruggedness and simplicity of operation coming from the compact and uncooled design of the instrument, make REFIR-PAD an ideal tool for the continuous, and possibly remote-operated, monitoring of the atmosphere from high-altitude ground stations.

[57] **Acknowledgments.** The authors want to acknowledge Francesco Castagnoli, of IFAC-CNR, for on-site technical support during the ECOWAR measurement campaign. This research was carried out with a grant from MIUR PRIN 2005, project 2005025202/Area 02, and funding from NASA grant NAG 513029. We are indebted to the Istituto di Fisica dello Spazio Interplanetario (INAF/IFSI), the Centro Nazionale di Meteorologia e Climatologia Aeronautica (CNMA), and the town of Valtournenche (Breuil-Cervinia) for logistic support at the two field sites of Plateau Rosa and Cervinia. Last, we would like to thank Marco Cacciani

of the Department of Physics, Laboratory for Remote Sensing of the Atmosphere, of the University of Rome "La Sapienza."

References

Bhawar, R., et al. (2008), Spectrally resolved observations of Earth's emission spectrum in the H_2O rotation band, *Geophys. Res. Lett.*, *35*, L04812, doi:10.1029/2007GL032207.

Bianchini, G., and L. Palchetti (2008), Technical Note: REFIR-PAD level 1 data analysis and performance characterization, *Atmos. Chem. Phys.*, *8*, 3817–3826.

Bianchini, G., L. Palchetti, and B. Carli (2006), A wide-band nadir-sounding spectroradiometer for the characterization of the Earth's outgoing longwave radiation, *Proc. SPIE Int. Soc. Opt. Eng.*, *6361*, 63610A.

Bianchini, G., L. Palchetti, A. Baglioni, and F. Castagnoli (2007), Far-infrared spectrally resolved broadband emission of the atmosphere from Morello and Gomito mountains near Florence, *Proc. SPIE Int. Soc. Opt. Eng.*, *6745*, 674518.

Bösenberg, J. (1998), Ground-based differential absorption lidar for water-vapor and temperature profiling, *Appl. Opt.*, *37*, 3845–3860.

Clough, S. A., M. J. Iacono, and J. L. Moncet (1992), Line-by-line calculations of atmospheric fluxes and cooling rates: Application to water vapor, *J. Geophys. Res.*, *97*, 15,761–15,785, doi:10.1029/92JD01419.

Clough, S. A., M. W. Shephard, E. J. Mlawer, J. S. Delamere, M. J. Iacono, K. Cady-Pereira, S. Boukabara, and P. D. Brown (2005), Atmospheric radiative transfer modeling: a summary of the AER codes: Short communication, *J. Quant. Spectrosc. Radiat. Transfer*, *91*, 233–244.

Delamere, J. S., S. A. Clough, V. H. Payne, E. J. Mlawer, D. D. Turner, and R. R. Gamache (2010), A far-infrared radiative closure study in the Arctic: Application to water vapor, *J. Geophys. Res.*, *115*, D17106, doi:10.1029/2009JD012968.

de Zafra, R. L., A. Parrish, P. M. Solomon, and J. W. Barrett (1983), A quasi continuous record of atmospheric opacity at λ = 1.1 mm over 34 days at Mauna Kea observatory, *Int. J. Infrared Millimeter Waves*, *4*, 757–765.

Di Girolamo, P., R. Marchese, D. N. Whiteman, and B. B. Demoz (2004), Rotational Raman Lidar measurements of atmospheric temperature in the UV, *Geophys. Res. Lett.*, *31*, L01106, doi:10.1029/2003GL018342.

Di Girolamo, P., D. Summa, and R. Ferretti (2009), Rotational Raman Lidar measurements for the characterization of stratosphere-troposphere exchange mechanisms, *J. Atmos. Oceanic Technol.*, *26*, 1742–1762.

Divakarla, M. G., C. D. Barnet, M. D. Goldberg, L. M. McMillin, E. Maddy, W. Wolf, L. Zhou, and X. Liu (2006), Validation of Atmospheric Infrared Sounder temperature and water vapor retrievals with matched radiosonde measurements and forecasts, *J. Geophys. Res.*, *111*, D09S15, doi:10.1029/2005JD006116.

Elliott, W. P., and D. J. Gaffen (1991), On the utility of radiosonde humidity archives for climate studies, *Bull. Am. Meteorol. Soc.*, *72*, 1507–1520.

England, M. N., R. A. Ferrare, S. H. Melfi, D. N. Whiteman, and T. A. Clark (1992), Atmospheric water vapor measurements: Comparison of microwave radiometry and lidar, *J. Geophys. Res.*, *97*, 899–916, doi:10.1029/91JD02384.

Fiorucci, I., et al. (2008), Measurements of low amounts of precipitable water vapor by millimeter wave spectroscopy: An intercomparison with radiosonde, Raman lidar, and Fourier transform infrared data, *J. Geophys. Res.*, *113*, D14314, doi:10.1029/2008JD009831.

Gordon, I. E., L. S. Rothman, R. R. Gamache, D. Jaquemart, C. Boone, P. F. Bernath, M. W. Shephard, J. S. Delamere, and S. A. Clough (2007), Current updates of the water-vapor line list in HITRAN: A new "Diet" for air-broadened half-widths, *J. Quant. Spectrosc. Radiat. Transfer*, *108*, 389–402, doi:10.1016/j.jqsrt.2007.06.009.

James, F. (1994), Minuit, function minimization and error analysis, reference manual, *D*506, CERN, Geneva, Switzerland.

Kiehl, J. T., and K. E. Trenberth (1997), Earth's Annual Global Mean Energy Budget, *Bull. Am. Meteorol. Soc.*, *78*, 197–208.

Kneizys, F. X., E. P. Shettle, W. O. Gallery, J. H. Chetwynd Jr., L. W. Abreu, J. E. A. Selby, R. W. Fenn, and R. A. McClatchey (1980), Atmospheric transmittance/radiance: Computer code LOWTRAN 5, *AFGL-TR-80-0670*, Air Force Geophys. Lab., Hanscom AFB, Mass.

Miloshevich, L. M., A. Paukkunen, H. Vömel, and S. J. Oltmans (2004), Development and validation of a time-lag correction for Vaisala radiosonde humidity measurements, *J. Atmos. Oceanic Technol.*, *21*, 1305–1327.

Niro, F., K. Jucks, and J.-M. Hartmann (2005), Spectral calculations in central and wing regions of CO_2 IR bands, IV: Software and database for the computation of atmospheric spectra, *J. Quant. Spectrosc. Radiat. Transfer*, *95*, 469–481.

Palchetti, L., A. Barbis, J. E. Harries, and D. Lastrucci (1999), Design and mathematical modelling of the space-borne far-infrared Fourier transform spectrometer for REFIR experiment, *Infrared Phys. Technol.*, *40*, 367–377.

Palchetti, L., G. Bianchini, F. Castagnoli, B. Carli, C. Serio, F. Esposito, V. Cuomo, R. Rizzi, and T. Maestri (2005), Breadboard of a Fourier-transform spectrometer for the Radiation Explorer in the Far Infrared atmospheric mission, *Appl. Opt.*, *44*, 2870–2878.

Palchetti, L., C. Belotti, G. Bianchini, F. Castagnoli, B. Carli, U. Cortesi, M. Pellegrini, C. Camy-Peyret, P. Jeseck, and Y. Té (2006), Technical note: First spectral measurement of the Earth's upwelling emission using an uncooled wideband Fourier transform spectrometer, *Atmos. Chem. Phys.*, *6*, 5025–5030.

Palchetti, L., G. Bianchini, B. Carli, U. Cortesi, and S. Del Bianco (2007), Measurement of the water vapour vertical profile and of the Earth's outgoing far infrared flux, *Atmos. Chem. Phys. Discuss.*, *7*, 17,741–17,767.

Rizzi, R., B. Carli, J. E. Harries, J. Leotin, C. Serio, A. Sutera, B. Bizzarri, R. Bonsignori, and S. Peskett (2001), Mission objectives and instrument requirements for the (REFIR) Radiation Explorer in the Far-InfraRed mission: An outline after the end of phase B0, in *Current Problems in Atmospheric Radiation*, edited by W. L. Smith and Y. M. Timofeyev, pp. 567–570, A. Deepak, Hampton, Va.

Rothman, L. S., et al. (2005), The HITRAN 2004 molecular spectroscopic database, *J. Quant. Spectrosc. Radiat. Transfer*, *96*, 139–204.

Serio, C., F. Esposito, G. Masiello, G. Pavese, M. R. Calvello, G. Grieco, V. Cuomo, H. L. Buijs, and C. B. Roy (2008), Interferometer for ground-based observations of emitted spectral radiance from the troposphere: Evaluation and retrieval performance, *Appl. Opt.*, *47*, 3909–3919.

Shephard, M. W., S. A. Clough, V. H. Payne, W. L. Smith, S. Kireev, and K. E. Cady-Pereira (2009), Performance of the line-by-line radiative transfer model (LBLRTM) for temperature and species retrievals: IASI case studies from JAIVEx, *Atmos. Chem. Phys.*, *9*, 7397–7417.

Sinha, A., and J. E. Harries (1995), Water vapour and greenhouse trapping: The role of far infrared absorption, *Geophys. Res. Lett.*, *22*, 2147–2150, doi:10.1029/95GL01891.

Smith, W. L., W. F. Feltz, R. O. Knuteson, H. E. Revercomb, H. M. Woolf, and H. B. Howell (1999), The retrieval of planetary boundary layer structure using ground-based infrared spectral radiance measurement, *J. Atmos. Oceanic Technol.*, *16*, 323–333.

Tobin, D. C., et al. (1999), Downwelling spectral radiance observations at the SHEBA ice station: Water vapor continuum measurements from 17 to 26μm, *J. Geophys. Res.*, *104*, 2081–2092, doi:10.1029/1998JD200057.

Vömel, H., H. Selkirk, L. Miloshevich, J. Valverde-Canossa, J. Valdés, E. Kyrö, R. Kivi, W. Stolz, G. Peng, and J. A. Diaz (2007), Radiation dry bias of the Vaisala RS92 humidity sensor, *J. Atmos. Oceanic Technol.*, *24*, 953–963.

Wang, J. Y. (1974), On the estimation of low-altitude water vapor profiles from ground-based infrared measurements, *J. Atmos. Sci.*, *31*, 513–521.

G. Bianchini and L. Palchetti, Istituto di Fisica Applicata "Nello Carrara," Consiglio Nazionale delle Ricerche, I-50019 Sesto Fiorentino, Italy. (gb@ifac.cnr.it)

P. Di Girolamo, Dipartimento di Ingegneria e Fisica dell'Ambiente, Università della Basilicata, I-85100 Potenza, Italy.

T. Di Iorio, Dipartimento di Fisica, Università di Roma "La Sapienza," I-00185 Roma, Italy.

I. Fiorucci and G. Muscari, Istituto Nazionale di Geofisica e Vulcanologia, I-00143 Roma, Italy.